JOURNAL OF Materials CHEMISTRY

Synthesis, microstructure and optical properties of ZnS films formed by electrostatic assisted aerosol jet deposition

B. Su† and K. L. Choy*

Department of Materials, Imperial College of Science, Technology and Medicine, Prince Consort Road, London, UK SW7 2BP. E-mail: k.choy@ic.ac.uk

Received 26th August 1999, Accepted 19th January 2000

ZnS films were synthesised using a novel electrostatic assisted aerosol jet deposition (EAAJD) technique at temperatures above 450 °C from an aqueous solution of zinc chloride and thiourea. The films showed a mixture of hexagonal and cubic structures and strong preferred orientations, with the *c*-axis normal to film surface. Annealing at higher temperatures improved the crystallinity of the as-deposited films. However, ZnO was formed when the as-deposited films were annealed in air. The ZnS films exhibit a planar structure with small crystal sizes (<200 nm). The optical direct bandgap values (3.35–3.46 eV) of the as-deposited films were lower than reported values for polycrystalline ZnS, probably owing to their poor crystallinity and partial oxidation.

Introduction

Zinc sulfide is a II–VI semiconductor with a wide direct bandgap (3.66 eV) in the near-UV region. It also shows transparency from the mid-IR through the visible region. ZnS thin films can be used in solar cell technology,[1] for electroluminescent displays,[2] as host matrices for quantum dot composites[3] and as multilayer dielectric filters.[4] ZnS thin films have been produced by a variety of vacuum and non-vacuum methods. Molecular beam epitaxy (MBE)[5,6] and metal–organic chemical vapour deposition (MOCVD)[7,8] are widely reported vacuum techniques. Non-vacuum techniques include chemical bath deposition,[9] successive ionic layer adsorption and reaction (SILAR),[10] spray pyrolysis[11,12] and atmospheric pressure chemical vapour deposition (APCVD) with high deposition rate.[13] The produced ZnS films possess different crystal structures and textures depending on the technique used and processing conditions.[11] We have developed a novel technique, called electrostatic assisted aerosol jet deposition (EAAJD), used for synthesising both oxide and non-oxide films, combining ultrasonic atomisation and electrostatic-assisted aerosol deposition.[14] In this technique, the precursor for ZnS deposition is atomised ultrasonically from an aqueous solution to form an aerosol, then the aerosol passes through a corona unit with the aid of a carrier gas. The charged aerosol is then directed towards the heated substrate under an electric field where it undergoes chemical reactions to produce solid films. The process operates in an open atmosphere, therefore, it is a low-cost process without the need for expensive vacuum equipment. The technique also demonstrates a high deposition efficiency and film growth rate because of the electrostatic discharge of the aerosol.[15] In this paper, the preparation of ZnS films by the EAAJD technique is reported. The microstructure and optical properties of the ZnS films are characterised.

Experimental

Zinc chloride ($ZnCl_2$) and thiourea [$(NH_2)_2CS$] aqueous solutions with molar concentrations of 0.01 to 0.05 M were used in the deposition. The apparatus used in the EAAJD process has been described in ref. 14. An electrostatic nozzle with electric potential of 5 to 15 kV was used. The aerosol was generated using an ultrasonic aerosol generator at a frequency of 1.7 MHz with nitrogen as the carrier gas. The gas flow rate was 2 l min^{-1}. The substrates used were optical glass slides. The deposition temperature was varied from 400 to 550 °C, and the deposition time from 1 to 10 min. Post-synthesis heat-treatment of the as-deposited film was performed in a quartz tube furnace with a controlled atmosphere to examine the effect of atmosphere on the film structure. Both nitrogen and air were used. The annealing temperature was 550 °C and the annealing time was 60 min.

The study of the decomposition of precursor was performed using simultaneous TGA–DTA apparatus (Stanton Redcroft STA-780) in a flowing air atmosphere (60 ml min^{-1}) at a heating rate of 10 °C min^{-1}. The precursor sample was prepared by evaporating the $ZnCl_2$ and thiourea aqueous solution. The sample mass used in the TGA–DTA measurement was 25 mg. A Philips PW1710 X-ray diffraction spectrometer (Cu-Kα radiation) was employed to study the phase and crystallinity of the films. The surface composition of the deposited films was characterised using X-ray photoelectron spectroscopy (XPS). The analysis was performed in a VG ESCALAB MkII instrument, with a base pressure of 5×10^{-10} Torr in the analysis chamber. 200 W Al-Kα radiation was used to excite the photoelectrons. Wide scanning was performed with the analyser operating at a constant pass energy of 100 eV. A JEOL 220T scanning electron microscope (SEM) was used to examine the surface morphology and cross-section of the films. Images were acquired using commercial software. A QUESANT atomic force microscope (AFM) was used to examine the surface morphology and grain size of the films. The optical properties of the films were measured using a Shimadzu UV-1601 spectrophotometer covering the spectral range from 200 to 800 nm.

Results and discussion

Thermal decomposition

The decomposition behaviour of the precursor for ZnS film deposition was studied using TGA–DTA (see Fig. 1). After an initial weight loss owing to the evaporation of H_2O at *ca.* 100 °C, decomposition starts at *ca.* 210 °C, leading to a rapid weight loss accompanied by both endothermic and exothermic

†Current address: IRC in Materials, University of Birmingham, Edgbaston, Birmingham, UK B15 2TT.

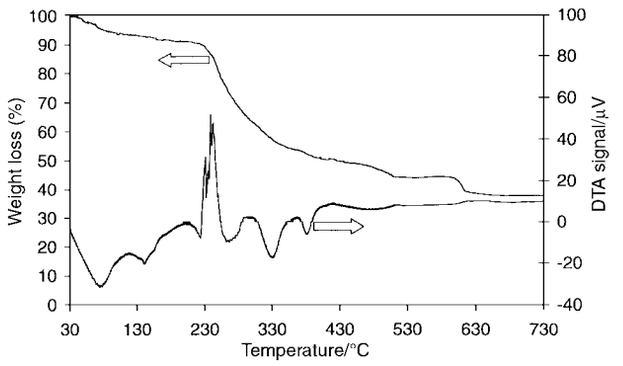

Fig. 1 TGA–DTA curve of the precursor used for ZnS film deposition.

reactions, as indicated in the DTA curve. The subsequent reaction at 330–400 °C is endothermic and the last weight loss at *ca.* 600 °C is accompanied by a small exothermic peak. The above observation is very similar to the thermal behaviour of dichlorobis(thiourea)cadmium, a precursor for CdS thin films.[16] In this work, a mixture of zinc chloride and thiourea in aqueous solution was used as the precursor for ZnS thin film deposition. Martin *et al.*[17] reported that a complex, dichlorobis(thiourea)zinc, was formed from the reaction of zinc chloride and thiourea in aqueous solution. The crystal structure of the complex was studied by Kunchur and Truter using X-ray crystallography.[18] In the molecule, each zinc atom is tetrahedrally co-ordinated to two chlorine and two sulfur atoms. Due to the similarity in molecular structure between dichlorobis(thiourea)zinc and dichlorobis(thiourea)cadmium, we may expect that their thermal decomposition behaviour will be similar. From the detailed investigation by X-ray diffraction and the evolved gas analysis (EGA)-FTIR,[17] the weight loss at temperatures between 210–400 °C involves a complete decomposition and rearrangement of the zinc complex to form ZnS. In the final stages (400–600 °C), slow oxidation may occur when the decomposition takes place in an oxidising atmosphere (*e.g.* air).

Crystallisation

Fig. 2 shows the XRD patterns of ZnS films before and after annealing at different temperatures under different atmospheres. Crystallisation starts at *ca.* 450 °C and only a single strong peak, at $2\theta = 28.9°$, is observed for the as-deposited films. This peak may be attributed to the hexagonal (002) and/or cubic (111) planes of ZnS. The absence of other diffraction peaks indicates a very strong preferred orientation, with the *c*-axis normal to the film surface, which was confirmed by the TEM investigation.[19] It is interesting to note that annealing the as-deposited films at 550 °C in different atmospheres resulted in different products. Weak peaks at $2\theta = 48.1$, 52.3, 56.6 and 59.2° can be assigned to the hexagonal (110) and/or cubic (220) planes, the hexagonal (103) plane, the hexagonal (112) and/or cubic (311) planes, and the hexagonal (004) and/or cubic (222) planes, respectively. These weak peaks appear when the amorphous film deposited at 400 °C was annealed at a higher temperature (*e.g.* 550 °C) in an N_2 atmosphere. This indicates that the annealed film is a mixture of hexagonal and cubic structures, but still maintains a strong preferred orientation. However, ZnO was formed when the as-deposited amorphous film was annealed in air. The peaks at $2\theta = 31.8$, 34.4, 36.3 and 47.6° correspond to the hexagonal ZnO (100), (002), (101) and (102) planes, respectively. The films became opaque when annealed in air, while films annealed in an N_2 atmosphere were transparent.

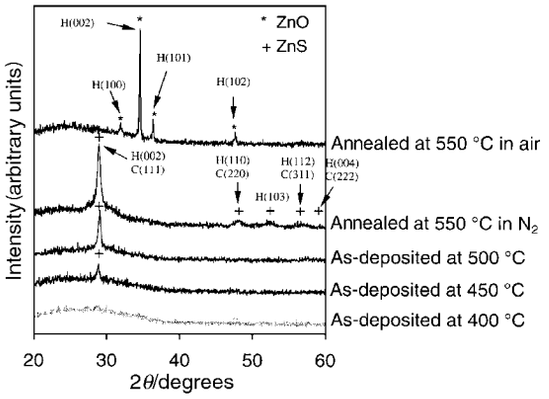

Fig. 2 XRD patterns of ZnS films before and after annealing at various temperatures under different atmospheres.

Surface composition

Fig. 3 shows the XPS wide scan from a film deposited at 500 °C. Apart from Zn and S, the major impurities found were C and O, with Cl as a minor impurity. The presence of C and O impurities may be due to the adsorption of CO_2 from the air and the residue from the precursor (thiourea) and water. The Cl impurity obviously comes from the zinc chloride precursor. As the deposition temperature increases, the C and Cl contents decrease, but O content increases. Quantitative analysis results show that the O content of the as-deposited films decreases after sputtering to remove the surface layer, and the Cl content remains almost the same. However, the films are still S-deficient and O-rich, which indicates that the oxidation may take place during deposition, as confirmed by the TGA–DTA results (see Fig. 1).

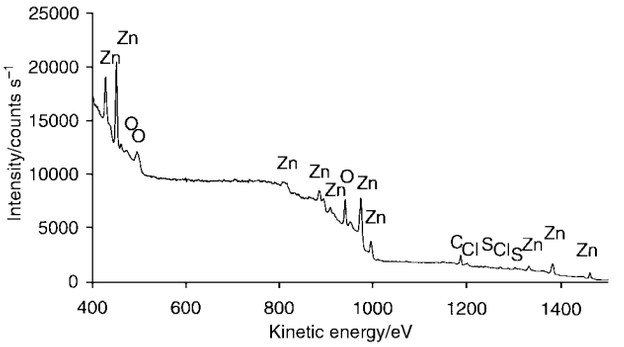

Fig. 3 XPS wide scan of a ZnS film deposited at 500 °C.

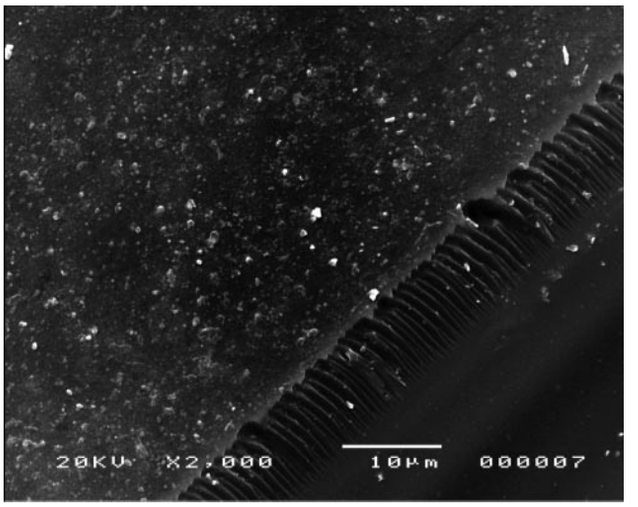

Fig. 4 SEM micrograph of a ZnS film deposited at 500 °C.

Microstructure

Fig. 4 shows the surface morphology and cross-section of a ZnS film deposited at 500 °C using the EAAJD technique. From the surface and cross-section, it appears that a dense and uniform film with good adhesion was obtained. The AFM images (Fig. 5) indicate that crystallites with very small grain sizes (<20 nm) were formed at a substrate temperature of 450 °C [Fig. 5(a)]. At substrate temperatures above 500 °C [Fig. 5(b and c)], the grain size increased rapidly (*ca.* 80–200 nm). Crystallinity was also improved, as shown by the XRD patterns (Fig. 2). TEM investigation showed that the ZnS crystals exhibit a planar structure with a straight-line boundary.[19]

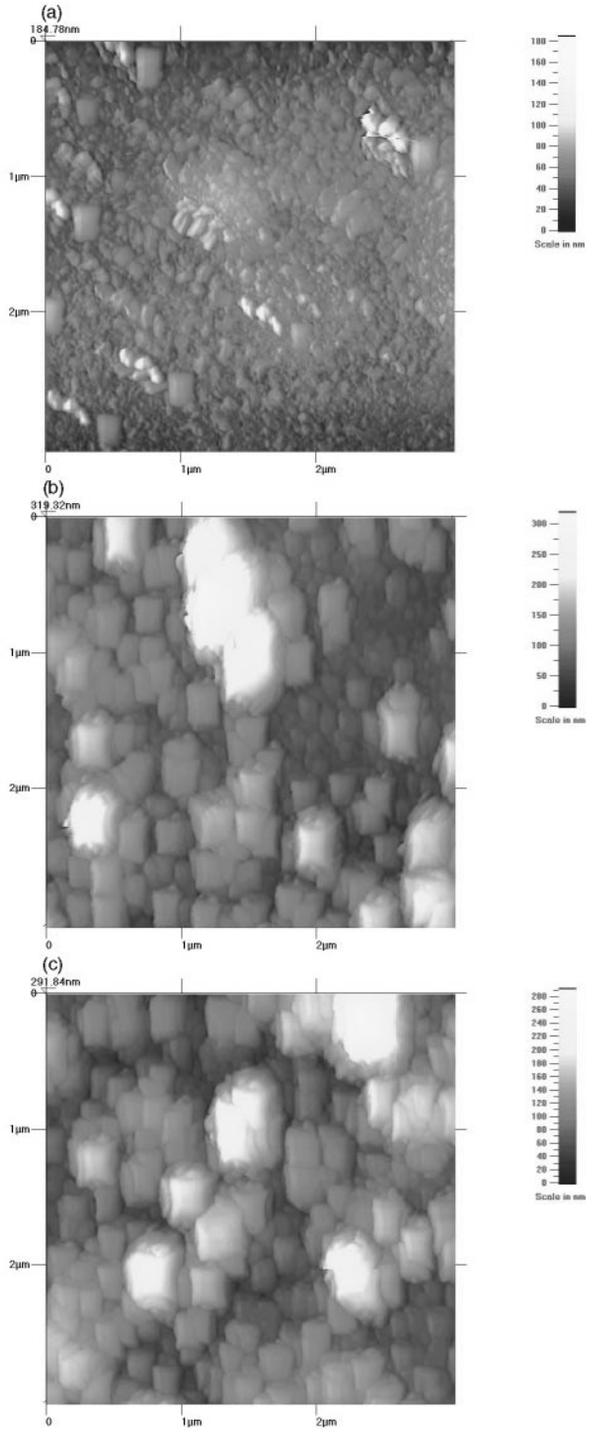

Fig. 5 AFM images of ZnS films deposited at different temperatures: (a) 450, (b) 500, (c) 550 °C.

Optical properties

Fig. 6 shows the absorption curves for ZnS films deposited at different temperatures. The optical energy bandgap, E_g, of the ZnS films was estimated from the optical measurements. From the film thickness, d, and the optical absorbance, A, the absorbance coefficient, α, was calculated using the Lambert law as follows:[20]

$$\ln(I_0/I) = 2.3A = \alpha d \quad (1)$$

where I_0 and I are the intensity of incident and transmitted radiation, respectively. The semiconductor bandgap, E_g, was determined by analysing the optical data with the expression for the optical absorbance, A, and the photon energy, $h\nu$, using eqn. (2):

$$A = k(h\nu - E_g)^{n/2}/h\nu \quad (2)$$

where k is a constant and n is a constant which is equal to 1 for a direct-gap material, and 4 for an indirect-gap material. The intercept of the plot of $(Ah\nu)^{2/n}$ *versus* $h\nu$ gives an estimate of E_g. The values of the direct bandgap, E_g, for the as-deposited ZnS films at deposition temperatures between 450 and 550 °C range from 3.35 to 3.46 eV, lower than those of polycrystalline cubic or hexagonal ZnS films ($E_g = 3.5$–3.6 eV) and close to the E_g value of amorphous ZnS ($E_g = 3.4$ eV).[21] The lower E_g may be attributed to the poor crystallinity of as-deposited ZnS films, as shown in the XRD patterns (Fig. 2), and partial oxidation of the film, as shown in the XPS analysis. In well-crystallised materials the electron transition is from band to band. However, in poorly-crystallised materials the electron transition may be from localised states at the valence band edge to extended states in the conduction band or *vice versa*.

Conclusions

Highly orientated ZnS films can be synthesised from an aqueous zinc chloride and thiourea solution using the electrostatic assisted aerosol jet deposition technique. Polycrystalline ZnS films are deposited at temperatures above 450 °C (using N_2 as a carrier gas) showing a mixture of cubic and hexagonal structures, but with poor crystallinity. Annealing at higher temperatures can improve the crystallinity of the films. However, a non-oxide atmosphere must be used, otherwise ZnO instead of ZnS will be formed. The ZnS films exhibit a planar structure with small crystal sizes (<200 nm). Optical measurements show that as-deposited ZnS films possess lower optical energy bandgap values (3.35–3.46 eV) than reported values for polycrystalline ZnS, probably owing to their poor crystallinity and partial oxidation.

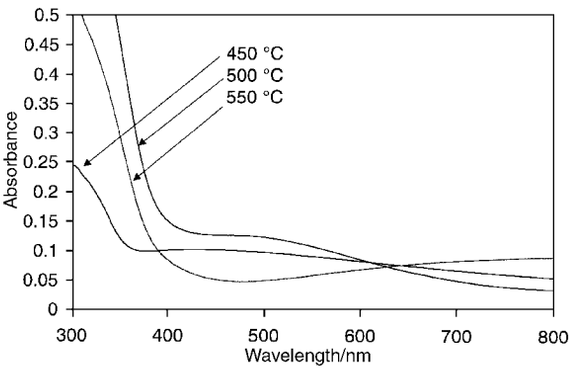

Fig. 6 Optical absorption curves for ZnS films deposited at different temperatures.

Acknowledgements

The authors wish to thank EPSRC-ROPA (GR/L73562) for financial support and Mr R. Willis for assisting with the optical characterisation.

References

1 T. L. Chu, S. S. Chu, J. Britt, C. Ferekides and C. Q. Wu, *Proceedings of the 22nd IEEE Photovoltaic Specialists Conference*, 1991, 1136.
2 T. Emma and M. McDonough, *J. Vac. Sci. Technol. A*, 1984, **2**, 362.
3 J. Rodriguez-Viejo, K. F. Jensen, H. Mattoussi, J. Michel, B. O. Dabbousi and M. G. Bawendi, *Appl. Phys. Lett.*, 1997, **70**, 2132.
4 A. M. Ledger, *Appl. Opt.*, 1979, **18**, 2979.
5 M. Yokoyama, K. I. Kashiro and S. I. Ohta, *Appl. Phys. Lett.*, 1986, **49**, 411.
6 S. Kaneda, S. Satou, T. Setoyama, S. I. Motoyama, M. Yokoyama and N. Ota, *J. Cryst. Growth*, 1986, **76**, 440.
7 S. Takata, T. Minami, T. Miyata and H. Nanto, *J. Cryst. Growth*, 1988, **86**, 257.
8 M. Nyman, M. J. Hampden-Smith and E. N. Duesler, *Chem. Vap. Deposition*, 1996, **2**, 171.
9 B. Mokili, Y. Charreire, R. Cortes and D. Lincot, *Thin Solid Films*, 1997, **288**, 21.
10 M. P. Valkonen, S. Lindroos, T. Kanniainen, M. Leskela, U. Tapper and E. Kauppinen, *Appl. Surf. Sci.*, 1997, **120**, 58.
11 R. D. Pike, H. Cui, R. Kershaw, K. Dwight, A. Wold, T. N. Blanton, N. A. Wernberg and H. J. Gysling, *Thin Solid Films*, 1993, **224**, 221.
12 H. H. Afifi, S. A. Mahmoud and A. Ashour, *Thin Solid Films*, 1995, **263**, 248.
13 I. P. Parkin, L. S. Price, A. M. E. Hardy, R. J. H. Clark, T. G. Hibbert and K. C. Molloy, *J. Phys. IV*, 1999, **9**, 403.
14 B. Su and K. L. Choy, British Patent Application No. 9900955.7, Jan. 1999.
15 B. Su and K. L. Choy, presented at the E-MRS Conference, Strasbourg, France, 1999, *Thin Solid Films*, in press.
16 M. Krunks, J. Madarasz, L. Hiltunen, R. Mannonen, E. Mellikov and L. Niinisto, *Acta Chem. Scand.*, 1991, **51**, 294.
17 F. J. Martin, H. Albers, P. V. Lambeck, G. M. H. Van de Velde and Th. J. A. Popma, *J. Aerosol Sci.*, 1991, **22**, S435.
18 N. R. Kunchur and M. R. Truter, *J. Chem. Soc.*, 1958, 3478.
19 M. Wei, B. Su and K. L. Choy, unpublished results.
20 A. Adachi, A. Kudo and T. Sakata, *Bull. Chem. Soc. Jpn.*, 1995, **68**, 3283.
21 A. Ashour, H. H. Afifi and S. A. Mahmoud, *Thin Solid Films*, 1994, **248**, 253.

Paper a906921f